Tracking the degradation of a PEMFC using a new accurate model.

Luis M. Perez[1,2], Samir Jemei[1], Loïc Boulon[2], Alexandre Ravey[3] and Javier Solano[4]
[1] Université de Franche-Comté, FEMTO-ST Institute, FCLAB, CNRS, F-90000 Belfort, France.
[2] Hydrogen Research Institute, Université Du Québec a Trois-Rivières, G8Z 4M3, Québec, Canada
[3]UTBM, CNRS, institut FEMTO-ST, F-90000 Belfort, France
[4]European Institute for Energy Research (EIFER), 76131, Karlsruhe, Germany

ABSTRACT – This article studies the degradation of a proton exchange membrane fuel cell (PEMFC), using a model-based technique. With this objective, a new accurate model is proposed and compared with a conventional model reported in the literature. This new model allows tracking the changes in the estimated parameters, reducing the variation and time computing compared to the conventional model. The behavior of the parameters is analyzed in the time based on a recent dataset through 1000 hours of operation. The results show that the proposed model could represent the PEMFC accurately, reducing the deviation standard of the estimated parameters by over 90%. Also, the estimated parameters of the proposed model show trends with respect the time. Those trends are analyzed to study their relation with PEMFC degradation.

Keywords – Fuel cell systems, PEMFC, Degradation, Model, Parameter.

1. INTRODUCTION

One of the main objectives in the fight against climate change is reducing the emissions of greenhouse gas in the systems that generate energy [1]. Among all the factors that contribute to climate change, the transportation sector has been identified as a significant source of greenhouse gas emissions [2]. Hydrogen-powered hybrid vehicles offer a potential solution to reduce carbon dioxide emissions from transportation [3]. The Proton Exchange Membrane Fuel Cell (PEMFC) has become a common solution as a generation source for transport and stationary applications because of its characteristics, including zero carbon dioxide emissions, low-temperature operation, a solid membrane between electrodes, high energy density, and other [4]. Despite all its advantages, the cost and service life of the PEMFC remains a barrier to the advancement of these systems [5]. As a way to improve these barriers, researchers are developing new methods for measuring the health state and forecasting the degradation of PEMFC to extend the remaining useful life (RUL) [6].

A PEMFC is an electrochemical device that has complex mechanisms for degradation [7]. Some works in the literature analyze the behavior of the PEMFC and its degradation mechanisms, therefore, fault detection and prognostics of the PEMFC is an active field of research [5].

Finding a model that represents the degradation of the different components in an accurate and precise way has been the objective of several works in the literature [8]. Nevertheless, the multi-physics simulation of the different systems that compose the PEMFC could drive into a model with a considerable number of parameters, high computational cost, and a problematic implementation [9]. Due to non-linearity, strong time-variation, and other characteristics that difficult obtain a physical model of PEMFC, numerous data-driven methods have been applied [10–15]. However, these methods often required a great quantity of data and involve a high computing burden for its application [9].

To face this problem, some works are developed hybrid methods that use semi-empirical models to emulate the behavior of the PEMFC and data-driven algorithm to predict the health state of the fuel cell (FC) [16–18]. Despite this, the focus of these articles is the prognostic, not the accuracy of the model or the comparison between different semi-empirical models. Some researchers investigated and compared different models of PEMFC and its applications [19]. However, the focus of this article is the comparison between the models regarding the error with the experimental data, but the accuracy and precision of the parameters obtained are not analyzed.

Other works in the literature like [20–23], employ meta-heuristic optimization algorithms to fit a conventional semi-empirical model to the experimental data. The aim of these articles is to compare the development of the optimization algorithm proposed and compared with other algorithms, taking reference to the sum of the squared errors (SSE). Despite this, in [20–23] the precision and accuracy of the estimated set of parameters are not analyzed.

Considering the above, this article develops a comparison between the proposed model and the conventional, taking as criteria the sum of the squared errors (SSE), the accuracy of the minimum find, and the precision of the estimated parameters. After, is developed an analysis of the estimated parameters over time to detect trends that reflect the degradation of the PEMFC.

The remaining part of the article is organized as follows: in section 2, presented the conventional model, the proposed model, the experimental data, and the optimization problem stated to fit the models. In the next section are shown the results for the comparison between both models and the analysis of the estimated parameters for the proposed model. Finally, a conclusion of the work is shown in section 4.

2. METHODOLOGY

The conventional model is a semi-empirical one frequently used to simulate the PEMFC under a polarization [24]. The common use of this model is due to the easy implementation in comparison with other models. This model represents the electrochemical behavior of one fuel cell, like a subtraction between the reversible voltage (E_{Nernst}) and three different loss factors: activation losses (V_{act}), ohmic losses (V_{Ohm}), and concentration losses (V_{con}). To represent the PEMFC stack, the model is scaled multiplying by the number of cells (N_{cells}) like is shown in (1) [24].

$$V_{stack} = N_{cells} \times (E_{Nernst} - V_{act} - V_{ohm} - V_{con}) \quad (1)$$

The reversible voltage (E_{Nernst}) is defined by (2) and depends on the temperature (T) and the partial inlet pressures of the hydrogen and oxygen, respectively (P_{H_2}, P_{O_2}).

$$E_{Nernst} = 1.229 - 0.85 \times 10^{-3} \cdot (T - 298.15) + 4.3085 \times 10^{-5} \cdot T \times \left[ln(P_{H2}) + \frac{1}{2} ln(P_{O2}) \right] \quad (2)$$

The three losses factors are represented by equations (3), (4), and (5).

$$V_{act} = -[\xi_1 + \xi_2 \cdot T + \xi_3 \cdot T \cdot ln\,(C_{O_2}) + \xi_4 \cdot T \cdot ln\,(I_{fc})] \quad (3)$$

$$V_{ohm} = I_{fc}(R_M + R_C) \quad (4)$$

$$V_{con} = -\beta \times ln\left(1 - \frac{J}{J_{max}}\right) \quad (5)$$

In the above equations, ξ_1, ξ_2, ξ_3, and ξ_4 are semi-empirical coefficients; C_{O_2} is the concentration of oxygen at the cathode surface; I_{fc} is the output current from the fuel cell stack; R_M and R_C are membrane and contact resistance, respectively; J is the current density and J_{max} is the maximum current density.

The proposed model in this work defines the stack voltage (V_{stack}) and the reversible voltage (E_{Nernst}) as the same in the conventional model. However, it introduces some simplifications regarding the activation, ohmic, and concentration losses defined by (6), (7), and (8).

$$V_{act} = \frac{RT}{2\alpha F} ln\left(\frac{J + J_{loss}}{J_0}\right) \quad (6)$$

$$V_{ohm} = J \times R_{eq} \quad (7)$$

$$V_{con} = -\beta_{eq} \times ln\left(1 - \frac{J}{J_{max}}\right) \quad (8)$$

In (6), R represents the constant of an ideal gas, F is the Faraday constant, J_0, J_{loss} and α are the exchange current density, lost internal current density, and the charge transfer coefficient, respectively. On the other hand, R_{eq} in (7) models the losses to transport ions and electrons; both are proportional to the current density level of the cell. Finally, β_{eq} in concentration losses is an adjusting coefficient like beta, but its limits are defined to increase the search region and improve the fitting.

2.1. *Experimental data*

To estimate the health state of the fuel cell, it is commonly employed the polarization test, which obtains experimental data called polarization curve (PC). PC is a graphic that describes the voltage of the fuel cell at a different level of current, and with constant operating conditions like temperature, pressures at the electrodes, etc. The experimental data used in this work are described and available in [25]. The experimental data is composed of 11 PCs that are shown in Fig. 1. Each PC is performed at intervals of 100 hours until 1000 hours of operation are reached. The operating conditions of all PCs are illustrated in Table 1.

2.2. *Optimization problem*

An inverse problem is posed to estimate the parameters that minimize the error between the model and the PC. The fitting process aims to minimize the SSE between the experimental voltage (V^{exp}) in the PC and the theoretical voltage calculated (V^{cal}) by the model. This is a typical least square problem where the experimental data fits the conventional and proposed model, each separately. The objective function to be minimized in the fitting process is expressed in (9).

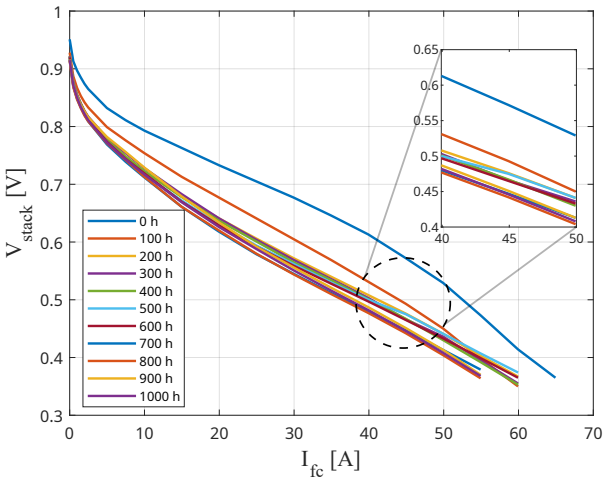

Fig. 1. Experimental polarization curves every 100 hours.

Table 1. Test conditions of the polarization curves.

Measurement variable	**Anode**	**Cathode**
Cell temperature $[K]$	$358,15$	
Stoichiometry factor	2	3.5
Relative humidity	50%	80%
Inlet pressure of electrodes [atm]	1.0856	1.0856
Cell activate area $[cm^2]$	25	
Thickness of membrane $[\mu m]$	15	
Maximum current $[A]$	80	

$$\min_{S \in \Delta} F_{obj} = \sum_{i=1}^{N} \left(V_i^{exp} - V_i^{cal}\right)^2 \quad (9)$$

In the above equation, N is the number of points of the polarization curve, and S is the mathematical set that contains the parameters of the model. Δ is the mathematical region delimited by the boundaries ($Lb \leq \varphi \leq Ub$) in Table 2 to the conventional and proposed model.

Table 2. Boundaries of the search region to the conventional and proposed model.

Variable (φ)	**Lower bound** (Lb)	**Upper bound** (Ub)
Conventional model		
ξ_1	-1.1997	-0.8532
ξ_2	1×10^{-3}	5×10^{-3}
ξ_3	3.6×10^{-5}	9.8×10^{-5}
ξ_4	-2.60×10^{-4}	-9.54×10^{-5}
λ	10	24
β	0.0136	0.5
R_C	1×10^{-4}	8×10^{-4}
Proposed model		
α	0.1	0.9
J_0	1×10^{-9}	1×10^{-2}
R_{eq}	1×10^{-5}	1
β_{eq}	1×10^{-5}	0.5
J_{loss}	1×10^{-5}	1×10^{-1}

To solve the optimization problem, Bald Eagle Search (BES) algorithm is used. This algorithm has shown promising results in parameter estimation of the PEMFC model [24]. This novel

nature-inspired meta-heuristic optimization algorithm is deeply described in [26].

3. RESULTS AND DISCUSSION

To analyze the variations in the objective function (SSE) and the set of estimated parameters, statistics criteria were calculated for the eleven PCs in the experimental data. For each PC, the optimization algorithm was executed 30 times to fit the parameters and calculates the fitting error (SSE). The purpose of the multiple executions is to calculate the variation of the SSE and the estimated parameters. These variations could be produced if exists multiple global minima in the solution region that affects the optimal point found by the optimization algorithm.

3.1. Comparative of the two worked models

An example of the results for the two worked models is shown in Fig. 2 for the PC taken at 0 hours of operation when the fuel cell is considered new. The mean of the SSE for the proposed and conventional model is $4.16\times^{-4}$ and $5.99\times^{-4}$, respectively. For the other PCs, a similar result of the SSE is achieved and illustrated in Table 3. The proposed model shows a lower SSE compared to the conventional model for all the PCs.

Regarding time computing, the proposed model has a mean of 30.11 s, compared to the conventional model with a mean of 46.96 s. It is worth mentioning that all the calculations were performed in Matlab software on a CPU i5-10505 with 32 GB of memory RAM.

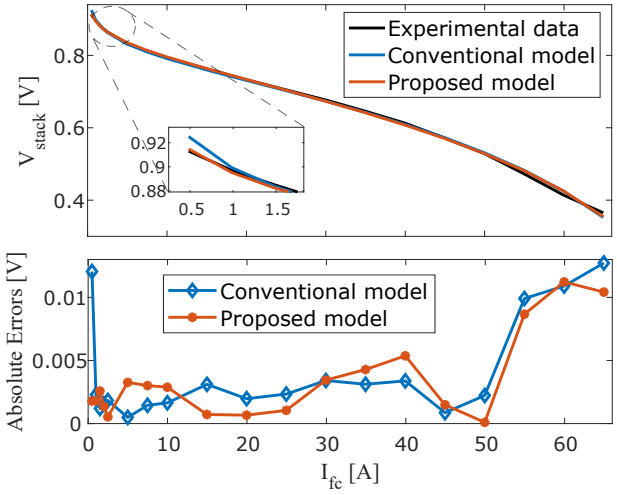

Fig. 2. Experimental and estimated polarization curve at 0 hours.

Table 3. Statistical results of the objective function for the eleven PCs.

Polarization test [hours]	Mean of SSE		Std. Deviation of SSE	
	Conventional model	Proposed model	Conventional model	Proposed model
0	5.99×10^{-4}	4.16×10^{-4}	4.02×10^{-18}	5.65×10^{-19}
100	6.33×10^{-4}	2.53×10^{-5}	1.19×10^{-18}	1.25×10^{-8}
200	1.54×10^{-3}	1.72×10^{-5}	1.56×10^{-18}	1.38×10^{-19}
300	2.02×10^{-3}	7.23×10^{-5}	1.82×10^{-18}	2.57×10^{-19}
400	1.79×10^{-3}	3.84×10^{-5}	1.26×10^{-18}	2.12×10^{-19}
500	2.47×10^{-3}	8.07×10^{-5}	1.45×10^{-18}	3.72×10^{-19}
600	2.62×10^{-3}	6.68×10^{-5}	1.59×10^{-18}	3.15×10^{-19}
700	2.22×10^{-3}	6.91×10^{-5}	1.39×10^{-18}	2.90×10^{-19}
800	1.97×10^{-3}	1.04×10^{-4}	1.66×10^{-18}	3.27×10^{-19}
900	2.16×10^{-3}	1.51×10^{-4}	1.72×10^{-18}	3.50×10^{-19}
1000	1.55×10^{-3}	3.75×10^{-5}	1.17×10^{-18}	2.50×10^{-19}

The variation of the estimated parameters was assessed with the relative standard deviation (RSD), defined by the ratio between the standard deviation and the mean of the parameter. The calculus of the RSD was established for each parameter of both models in the 11 PCs. For each PC, was selected the parameter with the maximal RSD, and the results are displayed in Table 4.

Table 4. Parameters with the maximum variation to both models.

PC [h]	Conventional model		Proposed model	
	Parameter	RSD	Parameter	RSD
0	ξ_1	1.37×10^{-1}	J_{loss}	1.63×10^{-7}
100	ξ_1	1.26×10^{-1}	J_{loss}	1.26×10^{-2}
200	ξ_1	1.32×10^{-1}	J_0	5.69×10^{-8}
300	ξ_1	1.38×10^{-1}	J_0	1.17×10^{-7}
400	ξ_1	1.35×10^{-1}	J_0	9.05×10^{-8}
500	ξ_1	1.27×10^{-1}	J_0	1.08×10^{-7}
600	ξ_1	1.31×10^{-1}	J_0	1.25×10^{-7}
700	ξ_1	1.28×10^{-1}	β_{eq}	3.12×10^{-2}
800	ξ_1	1.35×10^{-1}	J_0	1.56×10^{-7}
900	ξ_1	1.40×10^{-1}	β_{eq}	5.10×10^{-7}
1000	ξ_1	1.29×10^{-1}	J_0	1.11×10^{-7}

As shown in Table 4, the proposed model displays a maximum RSD of 6 orders of magnitude less than the conventional model for all the PCs, except the PC at 100 and 700 hours, where the differences are one order of magnitude. In the conventional model, the maximum RSD is presented in the parameter ξ_1 for all the PCs. The probability distributions of the parameter ξ_1 for the 11 PCs are shown in Fig. 3, where could be observed a standard deviation between 12.6% and 14% compared with the mean. These variations are due to the multiple combinations of parameters in the solution region of the conventional model, which generate the same global minimum value of the SSE.

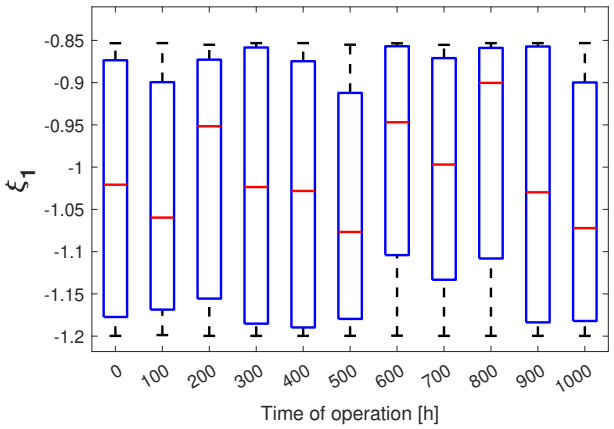

Fig. 3. Probability distribution of the estimated parameter ξ_1 for the conventional model.

The parameter ξ_1 was eliminated from the proposed model by redefining the activation losses, resulting in a lower variation of the estimated parameters for the proposed model as is illustrated in Table 4, and Fig 4. In Fig. 4, the probability distribution of β_{eq} can be found. β_{eq} is the parameter with the maximum variation for the proposed model. However, the maximum standard deviation of β_{eq} is approximately 3.12%, which is negligible compared to the mean value as shown in Fig. 4.

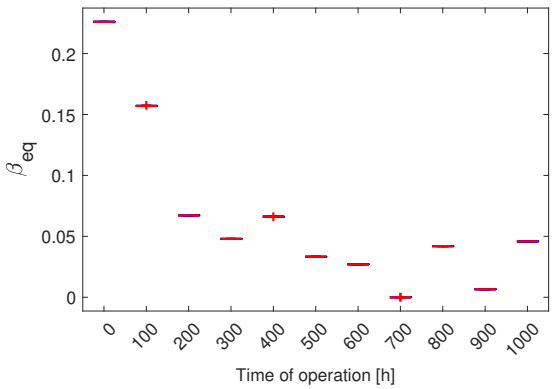

Fig. 4. Probability distribution of the estimated parameter β_{eq} for the proposed model.

3.2. *Parameters estimated*

The results observed in Table 4, Fig. 3 and Fig 4 indicate that tracking the changes at the time of β_{eq} is easier compared with ξ_1 due to the lower variation. Considering that the other parameters of the proposed model present a lower standard deviation compared with β_{eq}, this section analyzed the estimated parameters at the time for the proposed model. The average data of the five parameters estimated for the proposed model are shown in Fig. 5 for each PC.

As could be observed in Fig. 5, some of the five parameters as α, R_{eq}, and β_{eq} display a trend at the time. Due to the above, these three parameters are chosen to extract the trend component and represent the degradation in the activation, ohmic, and concentration losses. A parametric trend is calculated by fitting a function to the chosen parameters. Two different functions are fit to each parameter of the proposed model taking like the independent variable the time of operation in hours. The first is a simple linear trend that follows the function expressed in (10).

$$Y_{trend} = a + b \times t \tag{10}$$

Where, Y_{trend} is the trend component calculated, a and b are the parameters of the linear trend, and t is the time of operation. The second function used in the trend calculation is a root-square function stated in (11).

$$Y_{trend} = X_{ini} + c \times \sqrt{t} \tag{11}$$

In the above equation, X_{ini} is the value at 0 hours of operation, and c is the parameter of the trend function. For the two parametric functions used to calculate the trend component, the mean absolute error (MAE) is employed as a criterion for the fitting process. The linear and root-square trend component calculated for the three parameters of the proposed model are illustrated in Fig 6. The fitting error and statistical comparison of the two parametric trends for each parameter are presented in Table 5.

As suggested the Table 5 and Fig. 6, the root-square function achieves a lower MAE, MAPE, and RMSE for all the estimated parameters of the proposed model. For example, the MAPE of the root-square trend is 2.5%, 23.2%, and 13.7% lower than the linear trend, to the α, R_{eq}, and β_{eq}, respectively. Furthermore, the R_{eq} has the lowest MAPE between the chosen parameters with a 12.3%.

4. CONCLUSIONS

As a result of the comparison between the two models studied, it was found that the proposed model presents an SSE of at least 30% less than the conventional model. Also, reduce the variation in the estimated parameters by more than 90%

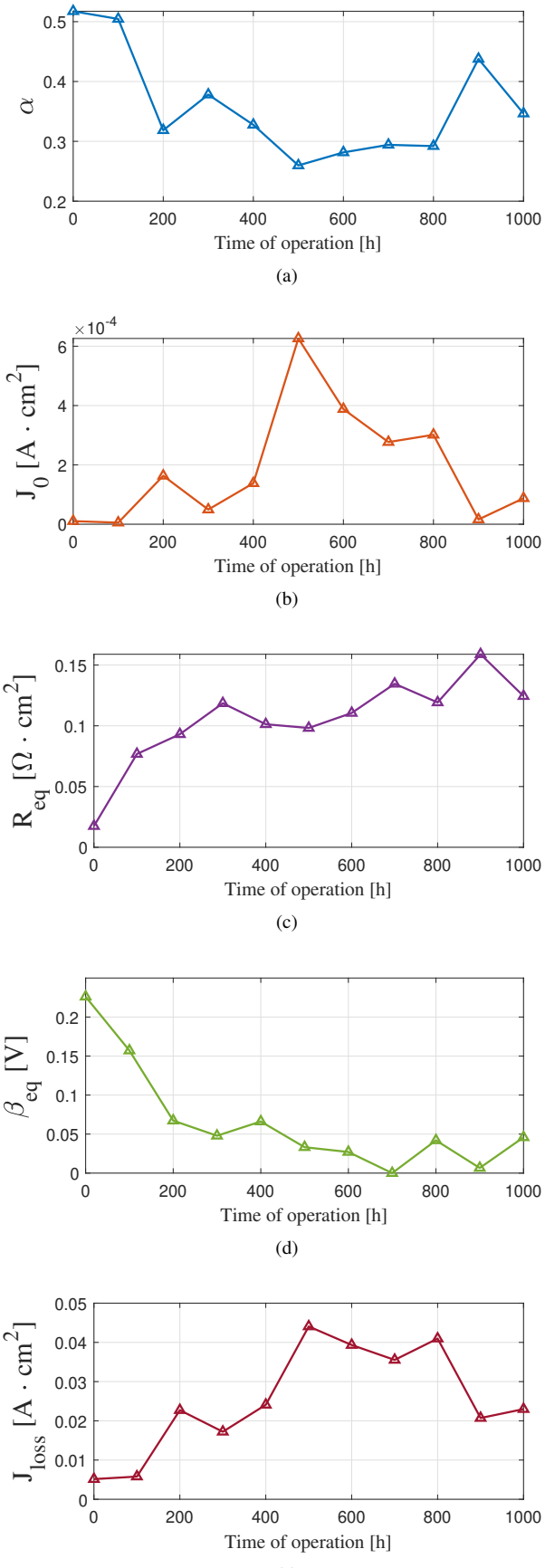

Fig. 5. Mean of estimated (a) α, (b) J_0, (c) R_{eq}, (d) β_{eq}, and (e) J_{loss} for the proposed model to all PCs.

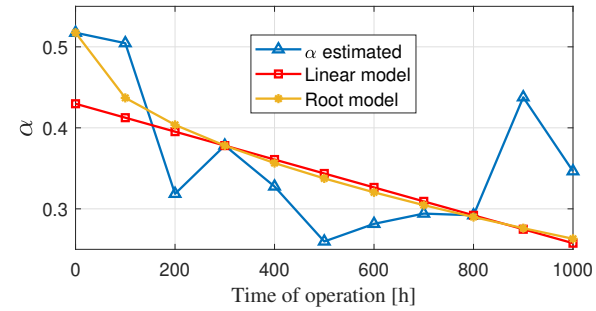

(a)

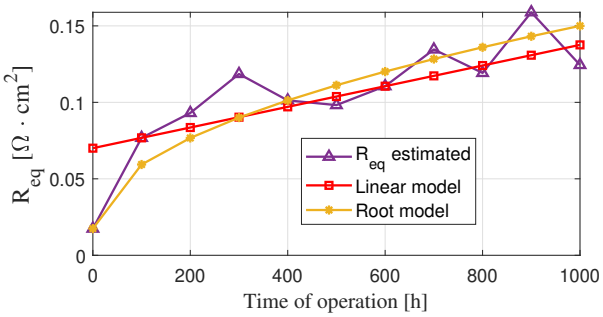

(b)

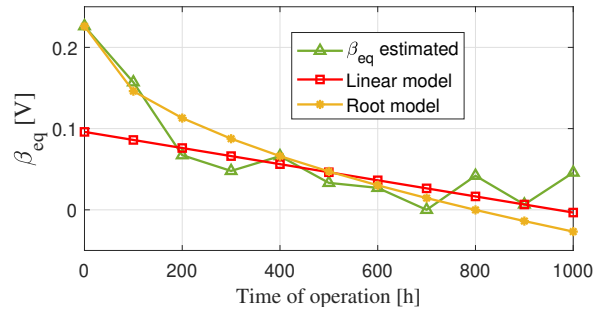

(c)

Fig. 6. Parametric trend component fitting to (a) α, (b) R_{eq}, (c) β_{eq} estimated.

for all the PCs, with a maximum relative standard deviation of 3.12×10^{-2}. The simplifications in the proposed model prevent that multiple sets of parameters generate the same value for the objective function. The above reduces the standard deviation of the estimated parameters and the computational burden without increasing the SSE. Additionally, some parameters of the proposed model show a clear trend over time and reflect the progressive degradation of the PEMFC. Hence, the proposed model could be used for supervision, prognostics, and health management strategies for PEMFC, especially in online applications.

Table 5. Fitting error for the two function trend to the estimated parameters of the proposed model.

Parameter estimated	Trend function	MAE	MAPE %	RMSE
$alpha$	Linear	0.0623	16.8860	0.0780
	Root	0.0505	14.3653	0.0697
R_{eq}	Linear	0.0149	35.5222	0.0213
	Root	0.0136	12.2991	0.0161
β_{eq}	Linear	0.0329	50.2944	0.0497
	Root	0.0239	36.5993	0.0326

5. REFERENCES

[1] IEA, "Towards hydrogen definitions based on their emissions intensity," International Energy Agency, Tech. Rep., 2023.

[2] T. Rudolf, T. Schurmann, S. Schwab, and S. Hohmann, "Toward holistic energy management strategies for fuel cell hybrid electric vehicles in heavy-duty applications," *Proceedings of the IEEE*, vol. 109, pp. 1094–1114, 2021.

[3] M. Kandidayeni, J. P. Trovão, M. Soleymani, and L. Boulon, "Towards health-aware energy management strategies in fuel cell hybrid electric vehicles: A review," *International Journal of Hydrogen Energy*, vol. 47, pp. 10 021–10 043, 2022.

[4] A. Jacome, D. Hissel, V. Heiries, M. Gerard, and S. Rosini, "Prognostic methods for proton exchange membrane fuel cell under automotive load cycling: a review," *IET Electrical Systems in Transportation*, vol. 10, pp. 369–375, 12 2020.

[5] H. Liu, J. Chen, D. Hissel, J. Lu, M. Hou, and Z. Shao, "Prognostics methods and degradation indexes of proton exchange membrane fuel cells: A review," *Renewable and Sustainable Energy Reviews*, vol. 123, p. 109721, 2020.

[6] C. Wang, Z. Li, R. Outbib, M. Dou, and D. Zhao, "Symbolic deep learning based prognostics for dynamic operating proton exchange membrane fuel cells," *Applied Energy*, vol. 305, p. 117918, 2022.

[7] T. Sutharssan, D. Montalvao, Y. K. Chen, W. C. Wang, C. Pisac, and H. Elemara, "A review on prognostics and health monitoring of proton exchange membrane fuel cell," *Renewable and Sustainable Energy Reviews*, vol. 75, pp. 440–450, 2017.

[8] H. Yuan, H. Dai, X. Wei, and P. Ming, "Model-based observers for internal states estimation and control of proton exchange membrane fuel cell system: A review," *Journal of Power Sources*, vol. 468, 8 2020.

[9] M. Yue, S. Jemei, N. Zerhouni, and R. Gouriveau, "Proton exchange membrane fuel cell system prognostics and decision-making: Current status and perspectives," *Renewable Energy*, vol. 179, pp. 2277–2294, 2021.

[10] A. Tang, Y. Yang, Q. Yu, Z. Zhang, and L. Yang, "A review of life prediction methods for pemfcs in electric vehicles," *Sustainability*, vol. 14, p. 9842, 8 2022.

[11] D. Xu, H. Qiu, L. Gao, Z. Yang, and D. Wang, "A novel dual-stream self-attention neural network for remaining useful life estimation of mechanical systems," *Reliability Engineering and System Safety*, vol. 222, 6 2022.

[12] B. Long, K. Wu, P. Li, and M. Li, "A novel remaining useful life prediction method for hydrogen fuel cells based on the gated recurrent unit neural network," *Applied Sciences (Switzerland)*, vol. 12, 1 2022.

[13] K. Chen, A. Badji, S. Laghrouche, and A. Djerdir, "Polymer electrolyte membrane fuel cells degradation prediction using multi-kernel relevance vector regression and whale optimization algorithm," *Applied Energy*, vol. 318, 7 2022.

[14] S. Zhang, T. Chen, F. Xiao, and R. Zhang, "Degradation prediction model of pemfc based on multi-reservoir echo state network with mini reservoir," *International Journal of Hydrogen Energy*, vol. 47, pp. 40 026–40 040, 12 2022.

[15] T. J. Chang, S. J. Cheng, C. H. Hsu, J. M. Miao, and S. F. Chen, "Prognostics for remaining useful life estimation in proton exchange membrane fuel cell by dynamic recurrent neural networks," *Energy Reports*, vol. 8, pp. 9441–9452, 11 2022.

[16] R. Ma, R. Xie, L. Xu, Y. Huangfu, and Y. Li, "A hybrid prognostic method for pemfc with aging parameter prediction," *IEEE Transactions on Transportation Electrification*, vol. 7, pp. 2318–2331, 2021.

[17] Z. Xia, Y. Wang, L. Ma, Y. Zhu, Y. Li, J. Tao, and G. Tian, "A hybrid prognostic method for proton-exchange-membrane fuel cell with decomposition forecasting framework based on aekf and lstm," *Sensors*, vol. 23, p. 166, 12 2022.

[18] Y. Wang, K. Wu, H. Zhao, J. Li, X. Sheng, Y. Yin, Q. Du, B. Zu, L. Han, and K. Jiao, "Degradation prediction of proton exchange membrane fuel cell stack using semi-empirical and data-driven methods," *Energy and AI*, vol. 11, 1 2023.

[19] L. Blanco-Cocom, S. Botello-Rionda, L. C. Ordoñez, and S. I. Valdez, "A

self-validating method via the unification of multiple models for consistent parameter identification in pem fuel cells," *Energies*, vol. 15, p. 885, 1 2022.

[20] R. Losantos, M. Montiel, R. Mustata, F. Zorrilla, and L. Valiño, "Parameter characterization of htpemfc using numerical simulation and genetic algorithms," *International Journal of Hydrogen Energy*, vol. 47, pp. 4814–4826, 1 2022.

[21] M. H. Qais, H. M. Hasanien, R. A. Turky, S. Alghuwainem, K. H. Loo, and M. Elgendy, "Optimal pem fuel cell model using a novel circle search algorithm," *Electronics (Switzerland)*, vol. 11, 6 2022, q2.

[22] Y. Chen and G. Zhang, "New parameters identification of proton exchange membrane fuel cell stacks based on an improved version of african vulture optimization algorithm," *Energy Reports*, vol. 8, pp. 3030–3040, 11 2022.

[23] R. Syah, J. W. G. Guerrero, A. L. Poltarykhin, W. Suksatan, S. Aravindhan, D. O. Bokov, W. K. Abdelbasset, S. Al-Janabi, A. F. Alkaim, and D. Y. Tumanov, "Developed teamwork optimizer for model parameter estimation of the proton exchange membrane fuel cell," *Energy Reports*, vol. 8, pp. 10 776–10 785, 11 2022.

[24] H. Rezk, A. Olabi, S. Ferahtia, and E. T. Sayed, "Accurate parameter estimation methodology applied to model proton exchange membrane fuel cell," *Energy*, vol. 255, p. 124454, 9 2022.

[25] J. Zuo, H. Lv, D. Zhou, Q. Xue, L. Jin, W. Zhou, D. Yang, and C. Zhang, "Long-term dynamic durability test datasets for single proton exchange membrane fuel cell," *Data in Brief*, vol. 35, p. 106775, 4 2021.

[26] H. A. Alsattar, A. A. Zaidan, and B. B. Zaidan, "Novel meta-heuristic bald eagle search optimisation algorithm," *Artificial Intelligence Review*, vol. 53, pp. 2237–2264, 3 2020.